Pergamon

Int. J. Solids Structures Vol. 34, No. 16, pp. 1985–2002, 1997

0020-7683/97 $17.00 + .00

PII: S0020-7683(96)00141-2

PLASTIC BENDING OF A RESIDUALLY STRESSED BEAM

A. M. KORSUNSKY and P. J. WITHERS
Department of Materials Science and Metallurgy, University of Cambridge, Pembroke Street, Cambridge, CB2 3QZ, U.K.

(*Received* 30 *April* 1996)

Abstract—This paper contains analysis of the bending beyond the elastic limit of an ideally elastic-plastic beam which contains a through-thickness distribution of high initial stresses. This is relevant to the analysis of service behaviour of components containing high residual stresses, such as might arise from heat treatment followed by quenching, plastic deformation induced by shot-peening, cold rolling, etc. The Timoshenko analysis of plastic bending of a beam is adapted for a particular case of a parabolic residual stress distribution typical of quenching treatment in bar or plate form. Attention is focused on the shake-down of residual stress, i.e., the variation in the residual stress and strain subsequent to bending. The implications of these results in terms of the analysis of bending tests are discussed. © 1997 Elsevier Science Ltd.

1. INTRODUCTION

Optimisation of the mechanical properties of many engineering alloys often requires thermal treatments which lead to strength improvements by precipitation hardening or phase transformation. In many cases this involves solution heat treatment at temperatures close to the alloy melting point, which is followed by quenching. Such treatments lead to the development of self-equilibrated systems of stresses within components, which play an important role in determining their service performance, especially under fatigue conditions (Cresdee *et al.*, 1993).

The motivation for the current analysis came from a series of experimental measurements of internal strains made using neutron diffraction. Specimens in the form of bars were machined from plates of a nickel-based superalloy, and ceramic particle reinforced aluminium alloy matrix composites. The bars were heat treated and quenched into oil and water, respectively, setting up high levels of self-equilibrating retained stresses, which in this paper will be referred to as *initial* stresses. The bars were subsequently fatigued in a four-point bending configuration. The purpose of the experimental strain measurements was to assess the shake-down of initial stresses in fatigue.

In this paper, plastic bending theory is used to analyse the evolution of one particular type of initial stress distribution: that which arises in materials due to quench treatment. This treatment is known to produce parabolic stress variation through the specimen thickness, when it is quenched in plate form (see Withers *et al.*, 1995). The wide applicability of this particular initial stress distribution is due to the fact that it is descried by the simplest (lowest order) function which allows both stresses and moments to be balanced. It is worth noting that in many practical situations the precise variation of the residual stresses is not known. Quite often the stresses can be estimated, directly or indirectly, at the specimen surface and somewhere in the bulk. Arguments of stress and moment balance then would suggest that it is natural to approximate such distributions by parabolae.

In this paper the initial stresses present within the material prior to bending are accounted for by introducing *position-dependent asymmetric yielding* into the model. This approach allows simple analytical solutions to be developed for the case of parabolic stress distributions. Due to the presence of initial stresses, the material response is asymmetric with respect to tension and compression, leading to premature yielding on the compressive side of the beam and causing a corresponding delay in the initiation of plastic flow on the tensile side. As a result, one-sided, or *unilateral* yielding takes place at moderate applied

moment levels, with the neutral axis of the beam shifting away from the centre of the cross-section. As the applied moment increases, further yielding may start to develop inwards from the tensile surface of the beam, or, for certain levels of initial stresses, even initiate *within* the beam thickness.

The phenomena outlined above are analysed and quantified in the following sections, and possible applications of the resulting framework to the interpretation of experimental data are outlined.

2. INELASTIC BENDING ANALYSIS

2.1. *Formulation*

Consider a beam of rectangular cross-section of width b and thickness $2h$, made of an elastic—ideally plastic material having Young's modulus E and yield stress σ_y. Pure bending of the beam in the vertical plane will be considered, with the through-thickness coordinate x measured from the mid-point. For the purposes of the analysis carried out in this paper all linear dimensions will be normalised with respect to the beam half-thickness h, so that the vertical position is given by the dimensionless parameter $\xi = x/h$. The stresses will also be normalised with respect to the material yield stress σ_y. The dimensionless parameters representing stresses will be denoted by τ, so that at a point ξ one finds $\tau(\xi) = \sigma/\sigma_y$. Further, it is convenient to normalise moments with respect to the *yield moment* of an initially unstressed beam, which is given by

$$M_y = \frac{\sigma_y I}{h} = \frac{2\sigma_y b h^2}{3}, \tag{1}$$

so that for the normalised moment $m = M/M_y$.

Let us assume that the beam is subjected to a parabolic *initial* stress profile characteristic of the quenching treatment which was performed in plate form. The initial stress profile is shown in Fig. 1(a). The distribution of the initial normalised stressed τ, is given by the equation (see Timoshenko and Goodier, 1965)

$$\tau_i(x) = q(1-3\xi^2). \tag{2}$$

Note the following features of this distribution:

(i) Initial stresses satisfy the conditions of stress and moment equilibrium within the cross-section. This initial stress profile may be fully determined from these conditions, given the value of the surface stress, based solely on the assumption of stress variation being parabolic.

(ii) Initial stresses are compressive near the surface of the beam ($|\xi| > 1/\sqrt{3}$); they reach a maximum magnitude of $-2q$ at the beam surfaces. The stresses are tensile in the central part of the beam ($|\xi| < 1/\sqrt{3}$), and reach the maximum of q at the beam centre.

(iii) Provided no yielding has occurred due to quenching treatment alone, the parameter q, which characterises the intensity of the initial stresses, varies within the range $0 \leqslant q \leqslant 0.5$.

Since the initial stress varies through the beam cross section, the yielding behaviour in tension or compression will obviously depend on position. For any chosen coordinate ξ within the beam cross-section, it is easy to determine the amount of tensile or compressive axial stress which may be applied in order to attain the condition of yielding at that point (as shown in Fig. 1(a) by solid arrows for tensile yielding and dashed arrows for compressive). The values are given by

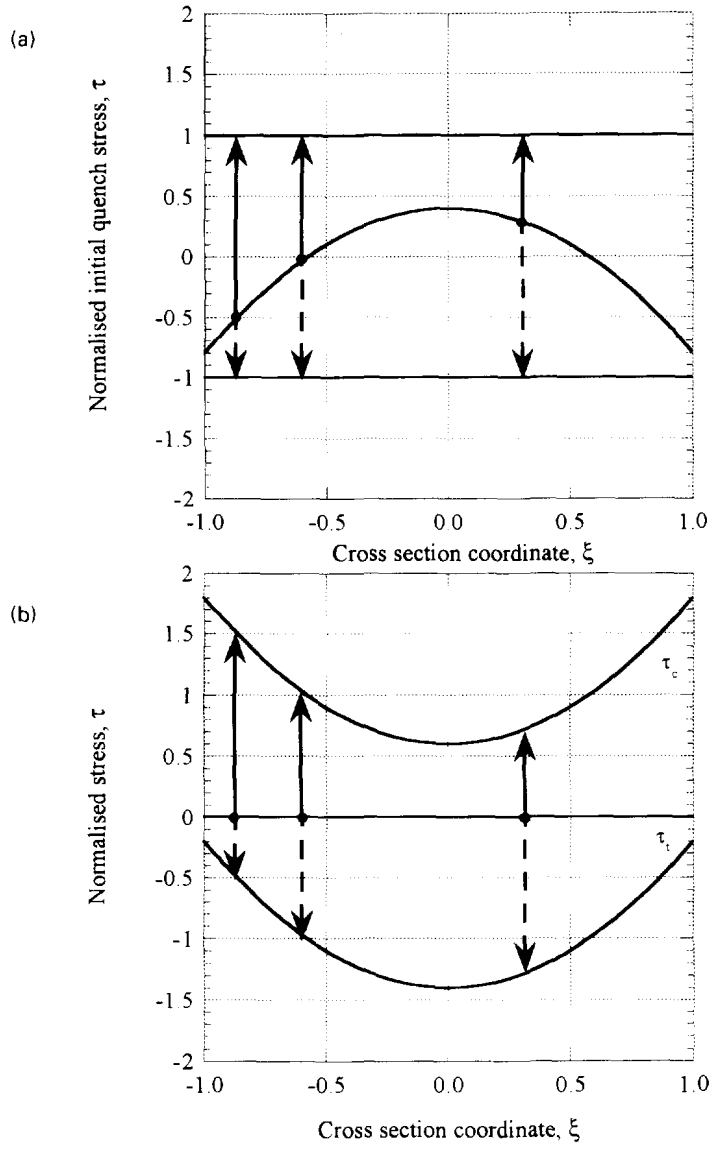

Fig. 1. (a) Initial stress profile, arising due to quenching treatment, and the variation of the distances from the tensile (——) and compressive (– – –) yield surfaces with position. (b) Asymmetric position dependent yield surfaces τ_t and τ_c.

$$\tau_t = 1 - q(1 - 3\xi^2), \tag{3}$$

$$\tau_c = -1 - q(1 - 3\xi^2), \tag{4}$$

where indices t and c indicate tension and compression, respectively.

It is proposed to use the following approach in order to account for this influence of the initial stresses present in the beam on the material's yielding behaviour. The initial stresses are assumed invariant throughout the loading history. Moreover, since these stresses satisfy both the force and moment equilibrium equations, they need not be considered at all during the stress analysis. However, the above equations indicate that the yield surface must be allowed to be position dependent and asymmetric with respect to the sign of the loading (tension/compression), to account for the influence of the initial stresses on yielding. This is depicted in Fig. 1(b), where the initial residual stresses have been collapsed onto the $\tau = 0$ line, while the upper and lower parabolae, given by eqns (3) and (4) above, indicate the modified tensile and compressive yield limits.

There are various perspectives from which the parameters which describe the state of bending and the yielding behaviour can be viewed. From the practical point of view, when the external moment is applied, the parameters such as the extent of plastic zones, beam curvature, etc., must be determined. However, it is instructive to reverse the order of consideration in order to develop an analytical model. Namely, the value of one parameter, such as the extent of the plastic zone, is assumed, and all others, including the applied moment, consistent with this extent of plasticity, are calculated in the course of solution.

Once the stress distribution within the beam which is caused by applying a given moment has been calculated, the process of elastic unloading is considered. The *additional* plasticity-induced residual stresses can be determined in this way. Finally, in order to estimate the shake-down of initial stresses caused by this loading cycle, the effect of these bending-induced residual stresses is superimposed on the initial parabolic quench stresses to obtain the final residual stress distribution.

2.2. *Unilateral yielding*

Let us start by considering an early stage of the loading cycle, when the applied moment is low, so that yielding has not occurred anywhere in the section. Under these conditions the beam behaves in a fully elastic manner. The neutral axis coincides with the cross-section centroid, and both strains and stresses vary linearly with the distance from the neutral axis, i.e. the coordinate ξ.

The beam then assumes a curvature $\kappa = 1/\rho$, where ρ is the bending radius, and the elastic strain ε varies through the section as (Timoshenko and Goodier, 1965)

$$\varepsilon = -h\xi/\rho. \tag{5}$$

Here the surface of the beam for $\xi = 1$ is considered to be in compression, and that for $\xi = -1$ is in tension, which leads to the negative sign in the above equation.

As the applied moment increases, the stress developed in the beam due to bending at point $\xi = 1$ becomes exactly sufficient to cause first yield at that point. This corresponds to

$$|\tau(1)| = 1 - 2q. \tag{6}$$

Thus, the normalised moment required for first yielding to occur is given by

$$m_{fy} = \frac{(1-2q)\sigma_y I}{hM_s} = 1 - 2q. \tag{7}$$

Upon further increase in the moment plastic yielding propagates into the cross-section from the compressive surface. For non-zero initial (quench) stresses, yielding initiates only on one side of the cross-section, and an asymmetric stress profile develops, causing the neutral axis to shift towards the tensile surface (Fig. 2).

Let us assume that as a result of yielding the plastic zone boundary lies a distance e from the centre of the beam cross section. The stress distribution arising in the beam must satisfy the following two criteria. Firstly, the stress must correspond to the yield limit throughout the plastic region. Secondly, within the elastic region the stress must remain proportional to the imposed strain, i.e. vary linearly.

The value of stress arising at the plastic zone boundary will be denoted by s. It is given by

$$s = \tau_s(e) = -1 - q(1 - 3e^2). \tag{8}$$

Our next step is to determine the normalised position of the neutral axis, denoted by c, as a function of e. In our analysis the neutral axis will be shifting from the cross-section centroid towards the tensile beam surface, which corresponds to negative values of c.

Within the elastic region, the stress $\tau(\xi)$ in Fig. 2 is given by

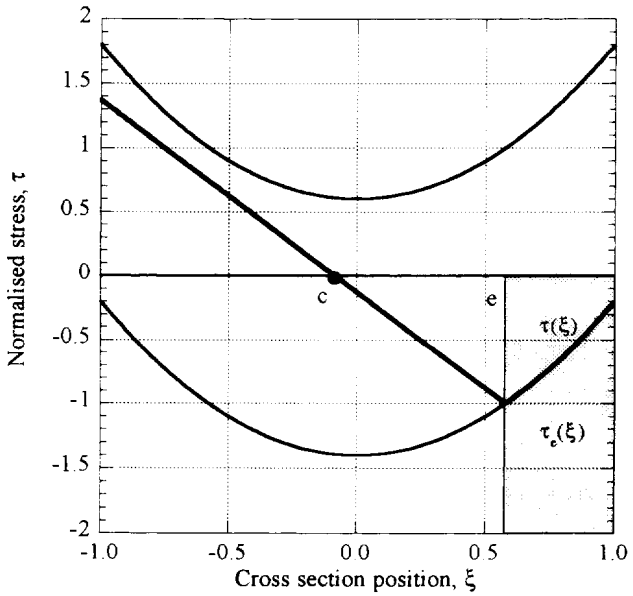

Fig. 2. Compressive plastic zone (shaded) in unilateral yielding. The plastic zone boundary is at $\xi = e$. The neutral axis position is $\xi = c$.

$$\tau(\xi) = s\frac{\xi - c}{e - c}, \quad \xi < e, \tag{9}$$

while in the plastic region

$$\tau(\xi) = -1 - q(1 - 3\xi^2), \quad \xi > e. \tag{10}$$

Let us now impose the requirement of stress balance across the beam cross-section, which, for the rectangular beam, is expressed in the form

$$\int_{-1}^{1} \tau(\xi)\, d\xi = 0. \tag{11}$$

Performing the simple integration, we obtain

$$-\frac{(1+c)^2}{2(e-c)}s + \frac{c+e}{2}s + \int_{e}^{1} [-1 - q(1-3\xi^2)]\, d\xi = 0. \tag{12}$$

Resolving this equation with respect to c leads to the result

$$c = e - \frac{[q(3e^2-1)-1](1+e)^2}{2\{[q(3e^2-1)-1](1+e) + eq(1-e^2) - (1-e)\}}. \tag{13}$$

This leads to the variation of the magnitude of c with e that is shown in Fig. 3 for $0.1 \leqslant q \leqslant 0.5$, indicating that while unilateral yielding persists the neutral axis moves progressively towards the tensile surface. The $q = 0$ curve cannot be included here, since no unilateral yielding occurs in this case.

Having determined the position of the neutral axis for any given extent of plastic zone (any value of e) and a range of values of the quenching stress magnitude q, we can proceed to calculate the moment. This is obviously given by

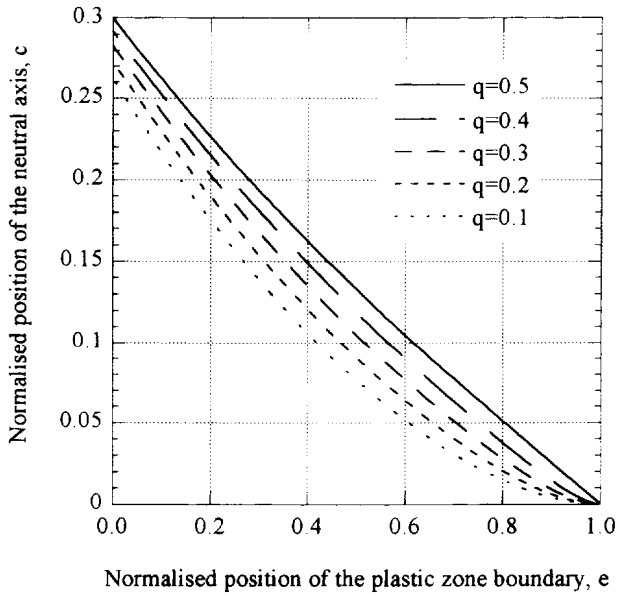

Fig. 3. Variation of the neutral axis position, c, with the position of the plastic zone boundary, e, in the unilateral yielding regime.

$$m = \frac{3}{2}\int_{-1}^{1} b\tau(\xi)\xi\,d\xi = \int_{-1}^{c} \frac{s(\xi-c)}{(e-c)}\xi\,d\xi + \int_{e}^{1} [-1-q(1-3\xi^2)]\xi\,d\xi. \tag{14}$$

Evaluating this expression we arrive at

$$m = \frac{s}{(e-c)}\left[\frac{1+e^3}{2} + \frac{3c(1-e^2)}{4}\right] - \tfrac{3}{4}(1+q)(1-e^2) - \tfrac{9}{8}q(1-e^4). \tag{15}$$

The variation of the normalised moment magnitude with the position of the plastic zone boundary e is shown in Fig. 4. As one would expect, for $q = 0.5$ yielding occurs for any non-zero moment, $m > 0$.

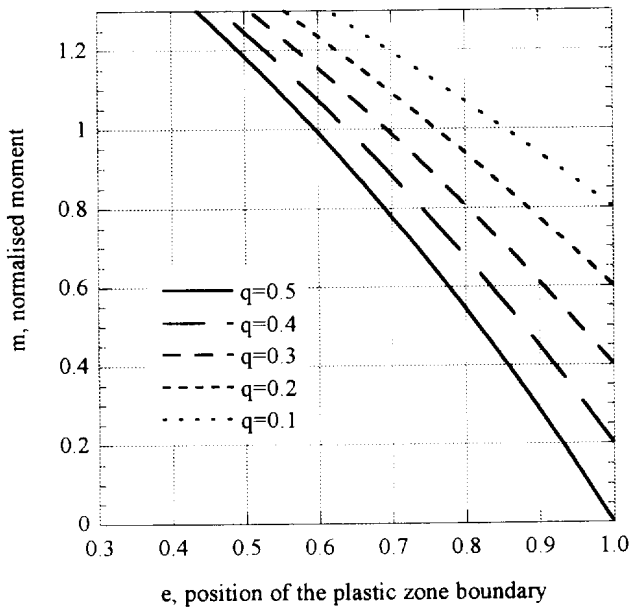

Fig. 4. Normalised moment, m, vs the position of the plastic zone boundary, e, in the unilateral yielding regime.

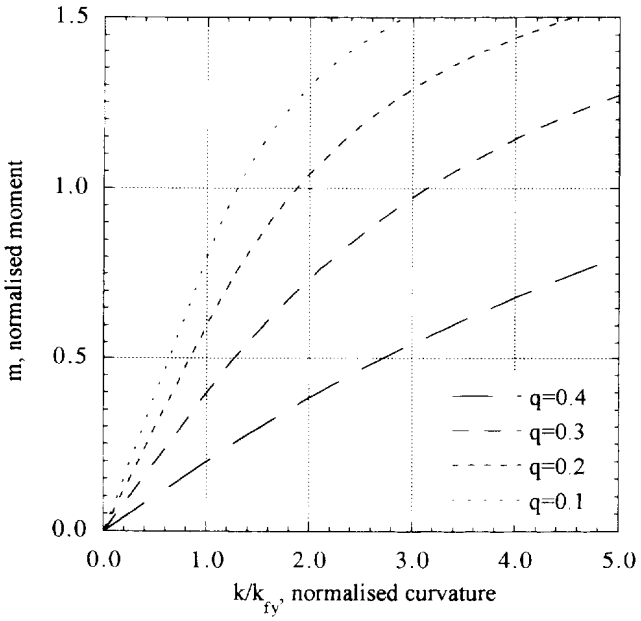

Fig. 5. The variation of the normalised moment, m, as a function of beam curvature in the unilateral yielding regime.

The curvature κ assumed by the beam when the plastic zone has advanced to e may now be determined as follows. The variation of strain ε throughout the cross-section is proportional to the linear distance from the neutral axis, $h(\xi - c)$, with the coefficient $-\kappa = 1/\rho$. Choosing the point on the plastic zone boundary, where the stress is given by s, we find

$$\kappa = \frac{\sigma_y}{Eh}\left|\frac{s}{e-c}\right|. \tag{16}$$

Note that the curvature at which first yielding takes place is easily found from the above by substituting $e = 1$, $c = 0$, $s = -1+2q$ into the above equation, so that

$$\kappa_{fy} = \frac{\sigma_y}{Eh}(1-2q). \tag{17}$$

For all values of curvature below κ_{fy} the beam remains fully elastic and a linear relationship between moment and curvature is maintained, which may be expressed in the following form:

$$m = (1-2q)\frac{\kappa}{\kappa_{fy}}. \tag{18}$$

As soon as κ exceeds κ_{fy}, plastic yielding leads to a lowering of the moment with respect to the fully elastic solution. In particular, this result implies that, for a given curvature, the bars with high initial stresses carry less moment than those with lower initial stresses, because plastic yielding occurs sooner. Conversely, residually stressed beams gain permanent shape changes due to bending at lower moments compared with unstressed beams. The moment-curvature diagrams, showing the variations of the normalised moment m vs normalise curvature κ/κ_{fy}, may be constructed using the results obtained above. They are shown in Fig. 5 for $q = 0.1$, 0.2, 0.3 and 0.4.

For practical applications the diagrams obtained in this section must be used in the reversed sense. This means that given a value of applied moment, the corresponding position of the plastic zone boundary e must be determined from Fig. 3, followed by the neutral

axis position c as a function of e from Fig. 4. Alternatively, the beam curvature may be found from Fig. 5 for any given value of normalised moment m.

2.3. *Limits of unilateral yielding*

In order to determine the limits of validity of the results obtained in the previous section, we need to predict the onset of yielding in tension. From Fig. 1(a), this phenomenon will first take place when the stress at some point within the elastic region reaches the corresponding tensile yield limit τ_t, which in most cases is likely to occur at the other surface of the beam. Geometrically, this corresponds to the line drawn from the point (e, s) via the point on the neutral axis $(c, 0)$ *touching* or *intersecting* the tensile yield surface τ_t at a certain value of $\xi < 0$. This line is given by eqn (9). It is not immediately obvious from either analytical or graphical representation of the problem which of the above two cases occurs first.

The case of the plastic zone propagating into the cross section from the tensile surface of the beam we will call the *bilateral* yielding regime (Fig. 6(a)).

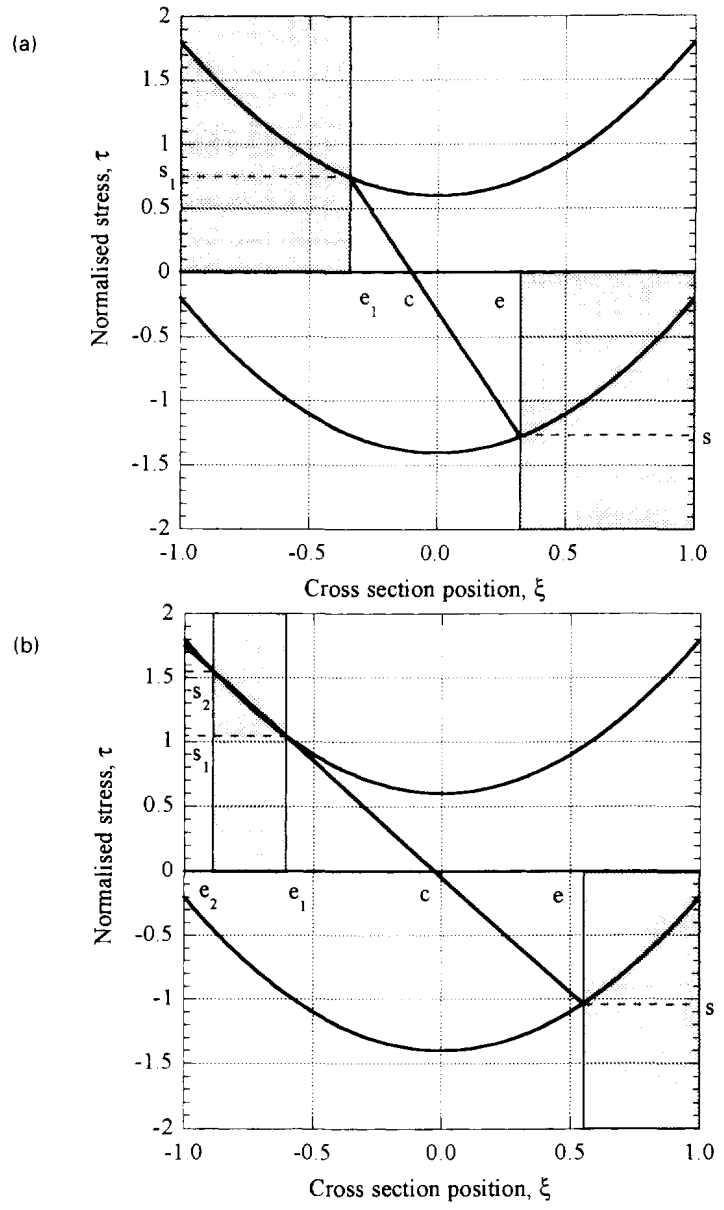

Fig. 6. (a) Stress variation in the bilateral yielding regime. (b) Stress variation in the internal yielding regime.

The case of touching at $\xi > -1$ corresponds to the interesting phenomenon of tensile yielding initiating *within* the beam. In this case, the plastic zone first initiates inside the cross section, and then expands inwards and outwards, until a configuration similar to bilateral yielding arises. We will call this case the *internal* yielding regime (Fig. 6(b)).

The condition for tensile yielding in tension to initiate at the specimen surface ($\xi = -1$) is given by

$$s\frac{-1-c}{e-c} = 1+2q, \tag{19}$$

from which we conclude that this mode of yielding imposes the following limit on the values of c for which the unilateral model is still applicable:

$$c(e) \leqslant c_1(e) = \frac{s+(1+2q)e}{1+2q-s}. \tag{20}$$

Obtaining a concise limit expression from the consideration of the competing *internal* yielding mode presents a somewhat more difficult problem. Points of intersection of the line (9) with the tensile yield surface τ_c are found from

$$s\frac{\xi-c}{e-c} = 1-q+3q\xi^2. \tag{21}$$

This leads to a quadratic equation for ξ, so that the condition of touching is given by the discriminant D of this equation being equal to zero.

$$D = \frac{s^2}{(e-c)^2} - 12q\left[(1-q) - \frac{sc}{e-c}\right] = 0. \tag{22}$$

The easiest way to resolve this equation is to recast it as a quadratic with the unknown $\eta = s/(e-c)$ with parameters, q, e, s,

$$\eta^2 + 12qe\eta - 12q(1+s-q) = 0. \tag{23}$$

Then, once the solutions for η are found in the form

$$\eta_{1,2} = -6qe\left(1 \pm \sqrt{1+\frac{(1+s-q)}{3qe^2}}\right), \tag{24}$$

the limiting values of c may be determined from

$$c_{1,2} = e - \frac{s}{\eta_{1,2}}. \tag{25}$$

However, even once $c_{1,2}$ are determined in this way, additional checks must be made to ensure that the corresponding touching points lie within the beam cross-section $\xi \geqslant -1$. A somewhat different approach will be used instead.

It is apparent from the above discussion that it is the competition between the two tensile yielding modes that determines the manner in which yielding develops with increasing applied moment.

In the next section, an assumption of bilateral yielding from the tensile surface is used, and further results are obtained for the parameters c, m, κ/κ_{fy}, etc.

In the subsequent section, a comparison is made between these results and a direct numerical simulation of the yielding process. This analysis will demonstrate that the assumption of bilateral yielding is valid for the vast majority of initial stress values and loading conditions, and leads to highly accurate results.

2.4. *Bilateral yielding*

Let us assume that as a result of the application of external moment plastic yielding has taken place in both compressive and tensile models, Fig. 6(a). The position of the plastic zone boundary in compression will be again denoted by $e_c = e$, with the stress given by

$$s = -1-q+3qe^2. \tag{26}$$

The position of the plastic zone boundary in tension will be denoted by e_t, with the corresponding stress given by

$$s_t = 1-q+3qe_t^2. \tag{27}$$

The location of the neutral axis will then be determined by the point on the line representing the stress variation within the elastic region, for which $\tau(c) = 0$. It is given, from Fig. 6(a), by the simple expression

$$c = \frac{s_t e - s e_t}{s_t - s}. \tag{28}$$

The expression for the stress at an arbitrary point within the elastic region may, after some simplifications, be given by

$$\tau(\xi) = 1-q+3qe^2 - \frac{2(\xi-e_t)}{(e-e_t)}. \tag{29}$$

The strategy of solution will be somewhat different in this case from the one used for unilateral yielding. Instead of focusing on the position of the neutral axis c, the boundary of the tensile plastic zone e_t will be chosen as the primary unknown, and c and further parameters will be determined afterwards using eqns (28), etc.

Since the stresses within the elastic region have now been expressed in terms of known parameters and e_t, and the stresses within the plastic regions are known to follow the respective yield surfaces, we may invoke the stress balance requirement once again in the form

$$\int_{-1}^{e_t} \tau_t(\xi) + \int_{e_t}^{e} \left[1-q+3qe^2 - \frac{2(\xi-e_t)}{(e-e_1)}\right] d\xi + \int_{e}^{1} \tau_c(\xi)\, d\xi = 0. \tag{30}$$

Evaluating the integrals and collecting the terms, we arrive at the following equation:

$$(e-e_t)[2-q(e-e_t)^2] = 4e. \tag{31}$$

This equation describes the dependence of e_t on the initial stress level q and the position of the compressive plastic zone boundary e. It is convenient to choose for the primary unknown in this equation not e_t itself, but its combination with e which corresponds to the extent of the elastic region, $\varepsilon = e-e_t$. Recasting it in the form

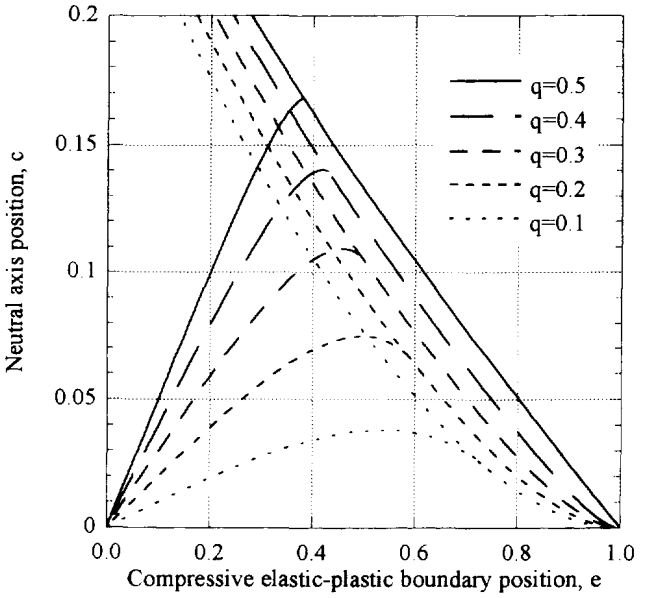

Fig. 7. Neutral axis position, c, vs the position of the compressive plastic zone boundary, e, in the bilateral and unilateral yielding regimes. For $q = 0$ only bilateral yielding occurs, represented by the line $c = 0$.

$$\varepsilon = \frac{4e}{2 - q\varepsilon^2}, \tag{32}$$

we obtain an equation which is amenable to effective numerical treatment. It can be solved recursively by assuming an initial trial value of $\varepsilon = \varepsilon_0$, $\varepsilon_0 > 0$ and substituting it into the right hand side to obtain the first approximation ε_1. Generally, using

$$\varepsilon_{n+1} = \frac{4e}{2 - q\varepsilon_n^2}, \tag{33}$$

where the subscript denotes the order of approximation, we obtain an algorithm which is convergent in all physically meaningful cases.

The resulting solutions for $c(e)$ are shown in Fig. 7, together with the unilateral yielding results. Note that the two solutions merge smoothly for all values of q. Note that the horizontal line $c = 0$ gives the solution corresponding to the case $q = 0$, since in this case the neutral axis coincides with the cross-section centroid for any size of plastic zone.

2.5. *Numerical simulation*

The results for all of the cases described above may be obtained from a simple numerical simulation routine. The flow chart describing the algorithm is shown in Fig. 8. The position of the compressive plastic zone boundary is varied in the range $0 \leqslant e \leqslant 1$. For any chosen value of e a trial value of the neutral axis position c is chosen from the range $-0.2 < c < 0$, and the resultant force transmitted through the cross-section is calculated. This involves a test which ensures that stresses at any point within the cross-section do not exceed the yield limits.

It is clear from Fig. 6(a) that if c^* denotes the true neutral axis position which provides stress balance, then the stress integral taken across the section is negative for all $c < c^*$ and positive for all $c > c^*$. Any numerical algorithm, for example, simple dichotomy, may be used to evaluate c with given accuracy using this property of the solution.

A comparison of the results obtained using this algorithm with those of the preceding sections shows that at $q > 0.3$ a slight deviation between the analytical results and the numerical simulation is observed at the junction of the unilateral and the bilateral yielding

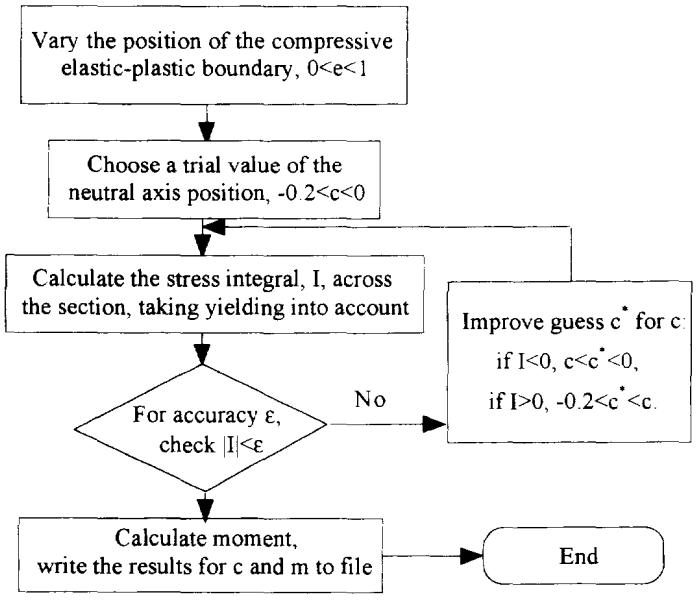

Fig. 8. Flow chart for the numerical algorithm used in the analysis.

regimes. An analysis of the plastic region boundaries shows that these deviations correspond to the *internal* yielding mode.

Figure 9 shows the transition between the unilateral and bilateral regimes for $q = 0.4$. The curve obtained using the numerical algorithm shows the correct values. It is clear from the graph that the bilateral solution leads to a very slight overestimate of the shift of the neutral axis position, c. The range of e for which the discrepancy is observed corresponds to the internal yielding regime. In this regime, the tensile plastic zone initiates within the beam section and expands rapidly (for a small change in e) both inwards and outwards, leading to the conditions assumed in the bilateral model. The evolution of the internal plastic zone in this regime is shown in Fig. 10 for $q = 0.4$ and $q = 0.5$. Note that the transition from unilateral to bilateral yielding regime via internal yielding happens over an extremely narrow range of values of e. Therefore, unless internal yielding is a matter of specific interest, it may be disregarded in the majority of practical cases.

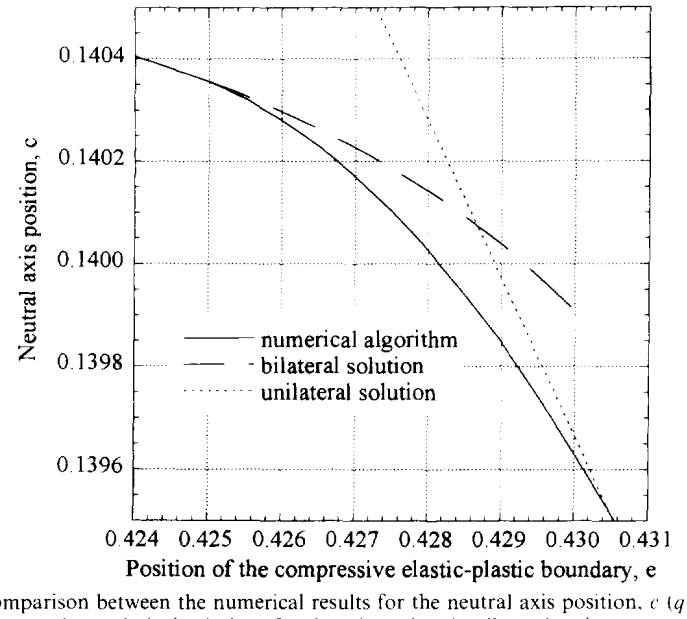

Fig. 9. A comparison between the numerical results for the neutral axis position, c ($q = 0.4$), and the analytical solutions for the bilateral and unilateral regimes.

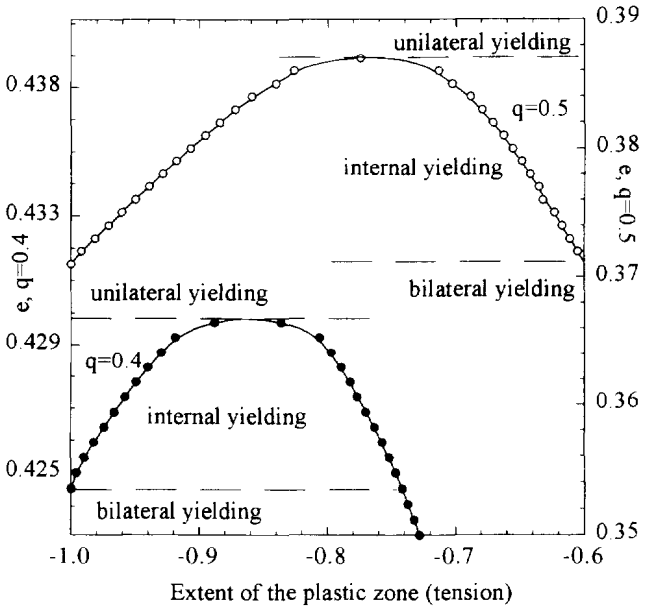

Fig. 10. Evolution of the tensile plastic zone as a function of the compressive plastic zone boundary position e.

It has been noted that from the practical viewpoint it is important to be able to determine all relevant variables given the applied moment and an estimate of the level of the initial stress. Figure 11 provides a master chart to be used for this purpose. For any given value of m and q, the position of the compressive plastic zone boundary, e, can be estimated using the curves given in the graph. The position of the neutral axis c may then be determined from Fig. 7. If the possibility of internal yielding is neglected, for the reasons suggested in the previous paragraph, the pair of values e, c will correspond either to the unilateral or to the bilateral regime. Which of the two regimes is realised can be determined depending on the branch of the curve $c(e)$. The rising branch (positive slope) corresponds to the bilateral regime, while the falling branch (negative slope) describes unilateral yielding. Once the yielding mode has been established, the stress profile can be easily calculated using the formulae from the corresponding section of this paper.

Finally, it is worth noting that the level of initial residual stresses may be estimated by monitoring the moment-deflection relationship, since a change in the specimen compliance takes place upon the onset of yielding.

3. RESIDUAL STRESS SHAKE-DOWN DUE TO BENDING

While there are very good mathematical reasons for dividing the stresses into initial and 'reaction' components, from an engineering viewpoint it is more helpful to divide them into permanent residual stresses and load related stresses. In order to evaluate the permanent effect of plastic bending on the residual stresses and strains within the beam, it is necessary to consider unloading from the maximum applied moment.

The results of the previous sections provide a framework allowing the determination of the stress profiles at any value of applied moment. Upon the removal of external load the beam unloads elastically, since the final residual stresses do not exceed the yield limit at any point, as will be confirmed in the subsequent analysis. The amount of unloading experienced by each point is linearly proportional to the distance from the section centroid, $\xi = 0$,

$$\tau_r = m\xi, \tag{34}$$

where m is the maximum normalised applied moment.

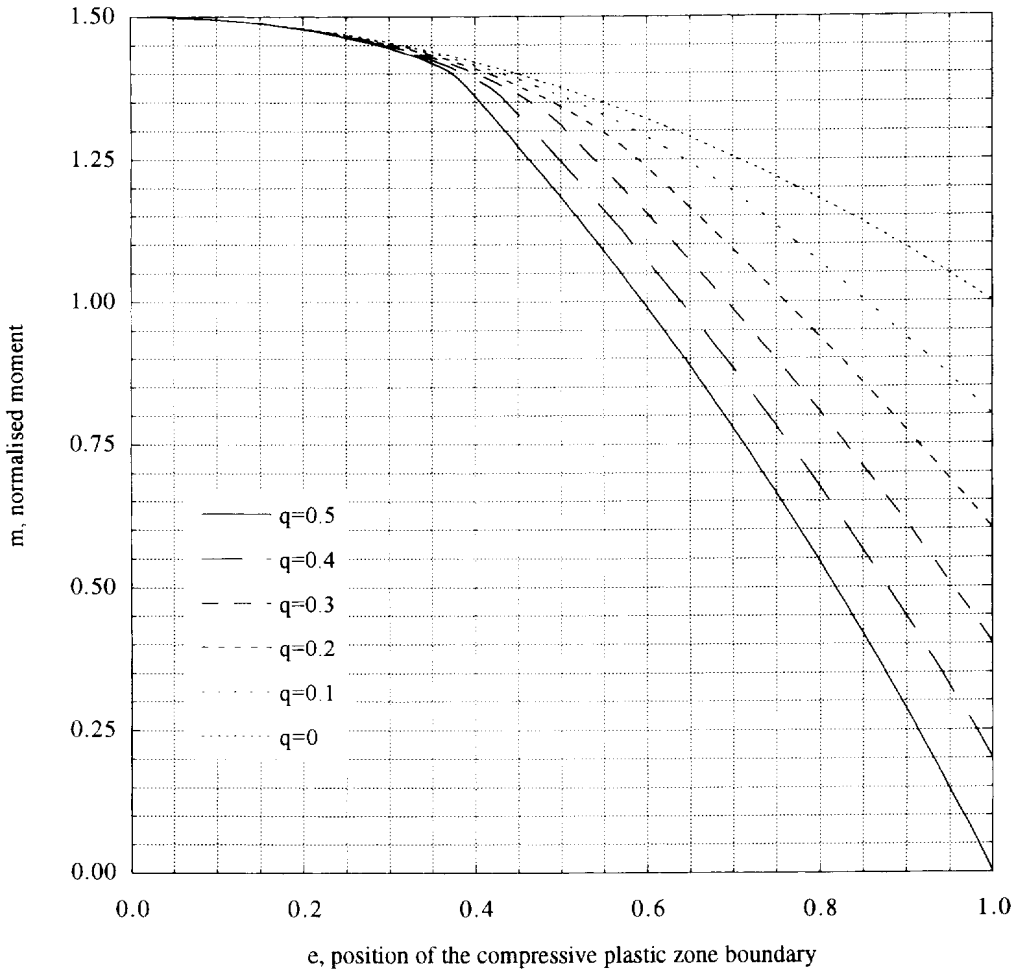

Fig. 11. Dependence of the position of the compressive plastic zone boundary on the normalised applied moment, m, and the quench stress level, q.

The process of elastic unloading from the maximum applied moment for the case of unilateral yielding is illustrated in Fig. 12(a) by the arrows which show how the stresses change as the applied bending moment is removed. The resulting stress profile τ_a represents the *additional* residual stresses developed in the beam due to bending.

In order to determine the final residual stress distribution, a combination of initial quench stress with the additional bending-induced stresses must be calculated. The final residual stress profile illustrates the plastic shake-down effect, and is shown in Fig. 12(b). Since once again full residual stresses are considered in this figure, the tensile and compressive yield limits are represented by the straight lines $\tau = 1$ and $\tau = -1$, respectively.

The final residual stress distribution consists of two regions. Within the region which remained elastic throughout the loading history, the stress variation is represented by a *modified parabola*. With respect to the initial stress profile, this parabola is shifted downwards and towards the surface that was bent in tension (Fig. 12(b)). The stress distribution is determined by the combination of three components: the initial quench stress, the 'reaction' stresses developing in the beam at maximum applied moment, eqn (9), and the elastic unloading. The resulting equation is

$$\tau(\xi) = q(1-3\xi^2) + s\frac{\xi - c}{e - c} + m\xi. \tag{35}$$

In contrast to this, in the region(s) which experienced plastic flow the residual stress profile is now given by a straight line. This line, which is shown short dashed in Fig. 12(b), has the

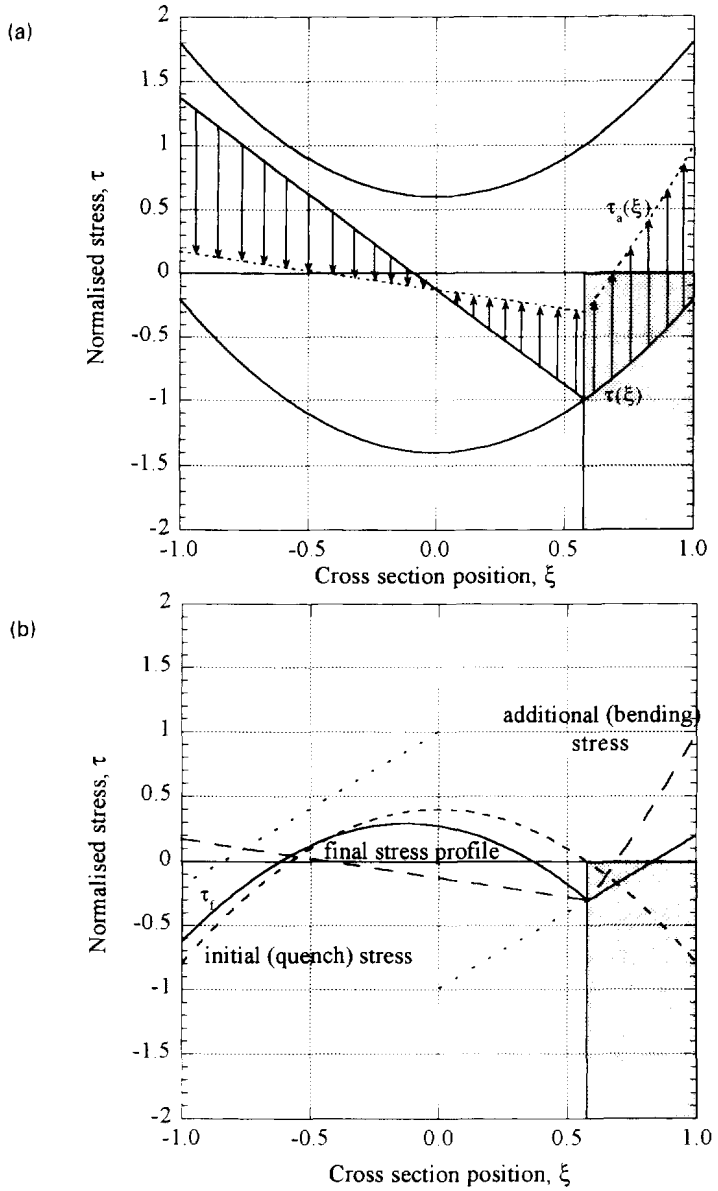

Fig. 12. (a) Stress profiles corresponding to yielding under maximum applied moment, $\tau(\xi)$, and the additional residual stress due to bending, $\tau_a(\xi)$, after elastic unloading, which is indicated by the arrows. (b) Initial (quench) and additional (bending) residual stresses, combined to produce the final residual stress profile $\tau_f(\xi)$ ($q=0.4$, $m=1.2$). (c) The final residual stress profile $\tau_f(\xi)$ arising after bilateral yielding ($q=0.4$, $m=1.4$). (d) The final residual stress profile $\tau_f(\xi)$ arising after bilateral yielding ($q=0.4$, $m=1.5$).

tangent which is equal to the maximum normalised applied moment, m. For $\xi = 0$, it passes through the point $\tau = -1$, so that its equation is given by

$$\tau(\xi) = m\xi - 1. \tag{36}$$

A similar line may be constructed for $\xi < 0$, so that

$$\tau(\xi) = m\xi + 1. \tag{37}$$

Note that this line lies everywhere above the *modified* parabola, provided no yielding in tension has taken place.

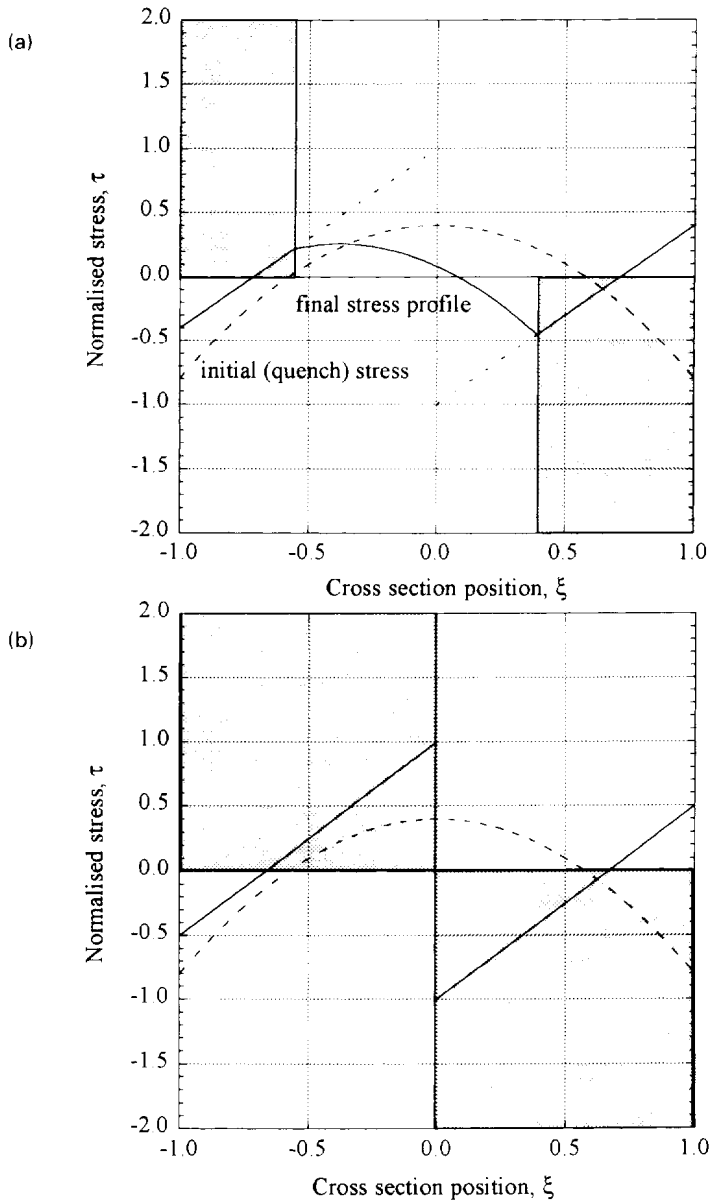

Fig. 12—*continued.*

The boundary between the two regions is determined by the intersection at point $\xi = e$ of the straight line (36), for the plastic region, and the *modified* parabola (35), for the elastic region.

Thus, unilateral plastic yielding leads to the shake-down of residual stresses throughout the beam cross section. In particular, at the compressive surface the stress varies from $-2q$ to $m-1$, while at the tensile surface the stress becomes equal to

$$-2q-m-s\frac{1+c}{e-c}.$$

Further increase in applied moment generally leads to bilateral yielding. The exception to this rule, namely, the internal yielding case, arises over a very narrow range of normalised applied moment, leading to a residual stress distribution which is virtually indistinguishable from the bilateral approximation.

The final residual stress profile arising upon unloading after bilateral yielding is shown in Fig. 12(c). Note that since yielding occurred both at the compressive and the tensile

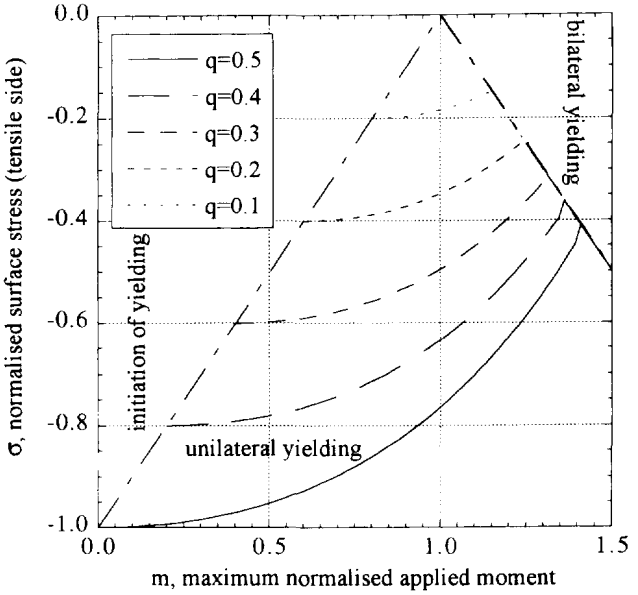

Fig. 13. Evolution of normalised residual stress at the tensile beam surface ($\xi = -1$).

surfaces, the stress variation follows the lines (36) and (37), respectively. In particular, the residual stresses at the compressive and tensile surfaces shake down to the values of $m-1$ and $1-m$, respectively.

Within the elastic region the stress variation remains parabolic, although the peak of the parabola shifts with respect to its initial position. The exact formula is constructed in a manner which is entirely analogous to the unilateral case, i.e. by summation of the relevant contributions from the initial quench stresses, the 'reaction' stress distribution at maximum applied moment, and the elastic unloading stresses.

The application of the maximum moment, $m = 1.5$, leads to yielding occurring throughout the section. The final residual stress profile is shown in Fig. 12(d). Complete shake-down of initial stresses has taken place, and the residual stress profile is indistinguishable from that of an initially unstressed beam.

From the above analysis, the residual stress at the compressive beam surface shakes down to the value of $m-1$, i.e. varies linearly with the maximum normalised applied moment, once the required for the initiation of yielding has been exceeded. The evolution of the residual stress at the tensile beam surface is shown in Fig. 13. After the onset of unilateral yielding, the stress follows one of the rising curves until the intersection with the straight line $\tau = 1-m$, when bilateral yielding takes place. Upon further increase in the applied moment the stress approaches the limiting value of -0.5 along the straight line.

Apart from the principal parameter e, which denotes the position of the compressive plastic zone boundary at maximum applied moment, a number of quantities which define the residual stress shake-down effect may be identified. One such quantity is the amount of change in the magnitude of stress on the compressive surface of the beam. Note that, as a result of plastic bending, the near-surface stress in this region may change sign and become tensile.

Also worthy of note is the change in the position and magnitude of the maximum tensile stress within the beam. The shift of the peak may be described in terms of a translation vector $\mathbf{v}$.

It is clear from the above analysis that all such characteristics of the final residual stress profile are determined by only two arguments: the maximum normalised applied moment m, and the initial stress level (quench intensity) q.

Based on this result, the following procedure may be adopted for the analysis of experimental measurements which involve plastic bending of residually stressed bars.

Firstly, let us suppose that, upon unloading the full stress profile through the bar thickness has been evaluated, for example, using such techniques as neutron diffraction or

synchrotron X-ray diffraction. The position of the plastic zone boundary at maximum load, e, may then be found as the point in the stress profile where it changes from linear to parabolic behaviour. Moreover, a special fitting function may be developed, which would consist of a parabolic section in the elastic region, and a linear function within the plastic zone. With the aid of this function, both the position of the plastic zone boundary e, and the leading coefficient of the parabola, $3q$, may be estimated. Using this estimate, the problem unknowns may be evaluated using the results presented in this paper. For example, the intensity of the quench stress can be found from Fig. 11, provided the value of maximum applied moment is known. Conversely, for known q the maximum moment can be evaluated using the same graph.

If the only information available is on the shake-down of the near-surface stresses, then the results of experimental measurements must be matched to the predictions of the analysis by trial-and-error. For example, for a known maximum applied moment, certain levels of initial stresses (q) must be assumed, and the surface stress shake-down calculated using the technique presented here. The guess for q must be improved, until satisfactory agreement has been achieved.

4. CONCLUSIONS

An analysis of inelastic bending of an initially stressed beam has been presented.

The results allow one to determine the mode of plastic yielding which occurs in pure bending. For any given level of the initial stresses due to quenching, the evolution of the plastic region(s), neutral axis position and beam curvature with increasing values of applied moment is predicted.

The shake-down of initial stresses is predicted by considering elastic unloading and evaluating the additional retained stress profile. The application of the results to improved analysis of experimental measurements is outlined.

Finally, a note should be made concerning the applicability of the model developed in this paper to materials which show substantial deviations from the ideally plastic behaviour assumed in the analysis.

If the material is work-hardening, a fully analytical treatment may turn out to be impossible. However, the numerical algorithm described in the previous section can be applied to obtain the dependence of the moment on the plastic zone extent, similar to the way it has been done in this paper. Work hardening increases the carrying capacity of the plastic regions, reducing both the extent of the plastic zone, $1-e$, and the shift of the neutral axis position, c, for a given value of the maximum normalised applied moment.

The model may also be modified and adjusted to allow the analysis of two-phase materials, such as metal matrix composites, for which only one of the phases can undergo yielding under the application of bending stresses. Assumptions concerning the load-sharing which takes place within the composite must be made.

Acknowledgement—A.M.K. wishes to thank EPSRC for their support during his work on this project.

REFERENCES

Cresdee, R. B., Edwards, W. J., Thomas, P. J. and Voss, G. F. (1993). Analysis of beam distortion during hot dip galvanising. *Materials Science and Technology* **9**, 161–167.

Withers, P. J., Clarke, A. P. and Fitzpatrick, M. E. (1995). Internal stress considerations during crack growth in Al/SiC particulate composites. In *Intrinsic and Extrinsic Mechanisms in Inorganic Composite Systems*, (eds J.J. Lewandowski and W.H. Hunt, Jr), The Minerals, Metals and Materials Society, Las Vegas, Nevada, 49–56.

Timoshenko, S. P. and Goodier, J. N. (1965). *Strength of Materials*, Prentice Hall, New York.